On the Size-Dependent Behavior of Nanocrystal−Ligand Bonds

Joshua Schrier* and Lin-Wang Wang

Computational Research Division, Lawrence Berkeley National Laboratory, Berkeley, California 94720

Received: February 21, 2006; In Final Form: April 18, 2006

Recent experiments have indicated that 3-mercapto-1-propanol ligands display a size-dependent binding energy of attachment to the surface of II−VI semiconductor nanocrystals. Using semiempirical calculations, we exhaustively calculate the energy of this bond at each surface site, for CdSe and CdSe/CdS core/shell nanocrystals ranging from 1.8 to 4.1 nm in diameter. Our results suggest that the experimentally observed changes in binding energy are due to the distribution of surface facets on the nanocrystals, and not related to the band gap, as proposed in the experimental paper.

I. Introduction

Colloidal semiconductor nanocrystals have been the subject of intense study, due to the unusual and size- and shape-tunable electrical, magnetic, and optical properties resulting from quantum confinement.[1] In addition, the nanocrystal surface is often passivated by a layer of organic ligands, which can play an important role in modifying both the optical properties[2] and the relative bio-compatibility[3] of these systems. Theoretical modeling of CdSe and CdS nanocrystal surface binding of molecules has focused primarily on alkyl phosphonic acids and amines, and their role in surface reconstruction, using methods ranging from force-field[4] calculations, semiempirical[5−7] and DFT[8,9] calculations on small clusters, and extrapolation from DFT calculations of binding to bulk facets.[10]

Recently, Aldana et al. performed acid titration experiments on 3-mercapto-1-propanol (MPOH) coated CdSe, CdS, and CdTe nanocrystals.[11] By observing a smaller pH value at which a well-mixed solution of nanocrystals precipitated out of solution (as a result of dissociation of the ligand−nanocrystal bond), it was determined that smaller nanocrystals have a stronger nanocrystal−ligand binding. Similarly, CdS, CdSe, and CdTe nanocrystals of the same sizes were found to precipitate at different pH values. Noting the ligand binding energy to be approximately inverse to the size and material dependence of the band gap, Aldana et al. proposed an explanation based on hard-soft−acid-base (HSAB) theory, which relates the difference (i.e., band gap) and the sum of the highest occupied, and lowest unoccupied, molecular orbital energies to the hardness and chemical potential, and therefore to the binding energy.[12] To study the origin of the size dependence in greater detail, in the present paper we examine the role of nanocrystal size on ligand binding by direct calculation of MPOH binding to each possible surface Cd site of the nanocrystal, using atomistic semiempirical calculations.

II. Computational Method

Wurtzite-structure CdSe nanocrystals were constructed with 1.8, 2.6, 3.4, and 4.1 nm diameters, removing surface atoms connected by only one bond to the remainder of the nanocrystal. The surface was then passivated by using hydrogen-like pseudoatoms of nuclear charge $Z = 0.5$ (for anions) and 1.5 (for cations) at each dangling bond site.[13−15] We note that the hydrogen-like passivation is used merely to remove the surface dangling bond states, while a MPOH molecule will be explicitly introduced to a given site. This scheme preserves the local charge neutrality of the system, capturing the essential characteristic of an ideal passivating agent, by removing the surface dangling bond states. For the CdSe/CdS core/shell nanocrystals, the valence force field method[16,17] was used to relax the geometry of the fully passivated nanocrystal. Both NMR and electrophoretic experiments performed by Aldana et al. indicate that the nanocrystal−MPOH complex is uncharged.[11]

The free energy measured experimentally includes both entropic and enthalpic terms. We neglect the entropic factors for the nanocrystal and ligand system, assuming the entropies are approximately the same whether the ligand is bound or unbound. Similarly, the free energy contributions of the dissociated MPOH and unbound pseudo-hydrogen ligand in solution will be independent of the size of the nanocrystal. For these reasons, we focus only on the relative values of the total (enthalpic) energy, by taking the difference between the total energy of the joined nanocrystal−ligand complex minus the total energy of the dissociated nanocrystal (without passivation by a pseudo-hydrogen at that site) and ligand. The total energies are obtained by using extended Hückel theory (EHT),[18,19] with a modified version of the Yaehmop package.[20] Although EHT does not give the quantitative agreement possible with more sophisticated methods, it is both capable of reproducing qualitative chemical properties and computationally amenable to the treatment of the hundreds of thousand-atom calculations required to examine ligand binding at each of the surface sites. Previous EHT calculations of small ($<$60 atoms) unpassivated CdSe and CdS nanocrystals by Gurin,[5,6] using the sp^3d^5 parametrization of Clementi and Roetii,[21] determined the contribution of the d orbitals to be small, thus in the present study we use only the minimal sp^3 valence Slater basis, with the standard parametrizations for Cd, Se, and S.[20] We also note that Cerdá and Soria have devised a parametrization fit to the bulk properties of Cd, using an sp^3d^5 basis.[22]

Since the use of the pseudo-hydrogen atoms is not standard, we will define their parametrization in the EHT model. In EHT the diagonal terms of the Hamiltonian are determined by the ionization potential, IP, of the atomic species, which for the pseudo-hydrogen ligands is

$$\mathrm{IP} = (-13.6\ \mathrm{eV})Z_{\mathrm{eff}}{}^2 \qquad (1)$$

10.1021/jp061117y CCC: $33.50
Published on Web 05/26/2006

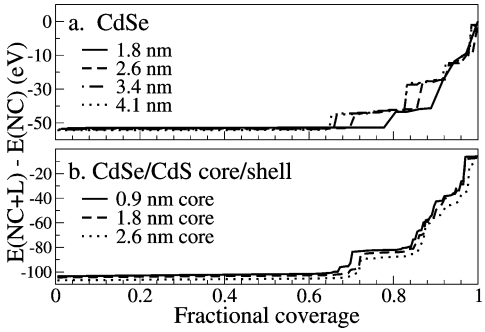

Figure 1. (a) Binding energy for CdSe nanocrystals of varying diameter. (b) Binding energy for CdSe/CdS core/shell nanocrystals, with total diameter fixed at 4.1 nm, and with the diameter of the core varied. In both cases, the larger nanocrystals have a more negative (stronger binding) value of the low-energy plateau.

For the $Z = 1.5$ ligand, we used the reduced (following Slater's rules) effective nuclear charge $Z_{\text{eff}} = (Z - 0.3)$ to evaluate the ionization potential, to account for the partial screening of the nuclear charge by the other electron, and thus prevent it from becoming unphysically large. The off-diagonal Hamiltonian matrix elements are proportional to the overlap between the atomic orbitals. Thus, parametrization for the pseudo-hydrogen ligands consists of determining the coefficients for the single Slater s-orbitals

$$\psi_{nlm}(r,\theta,\phi) = Nr^{c}e^{-\xi r}Y_{m}^{l}(\theta,\phi) \qquad (2)$$

For a hydrogen atom, $c = 1.0$, and following Slater's rules, $\xi = (Z - 0.3)/a_0$. Consequently, the parameters are $\xi_{0.5} = 0.378$ Å^{-1}, $\text{IP}_{0.5} = -3.4$ eV, and $\xi_{1.5} = 2.268$ Å^{-1}, $\text{IP}_{1.5} = -19.584$ eV.

Starting with the fully pseudo-hydrogen-passivated nanocrystal, the total energy evaluation is performed by removing a single pseudo-hydrogen ligand, and replacing it with a MPOH ligand. The difference between the total energy of the NC with the attached ligand and the NC without the attached ligand and pseudo-hydrogen at that site is repeated for each surface Cd site, and ordered from lowest to highest to generate the plots of Figure 1. This procedure does not examine the role of possible cooperativity effects between the binding of neighboring ligands, which were observed in DFT calculations of the binding of amines to the wurtzite 0001 face of CdSe.[10]

III. Results and Discussion

We began our study with an examination of CdSe nanocrystals, since the experiment of Aldana et al.[11] indicated CdSe to have the largest size-dependent change in the nanocrystal−ligand binding free energy. The results of our calculation are depicted in Figure 1a; as discussed in the previous section, our interest is only in the relative energies between the bound and unbound nanocrystal−ligand complexes, ignoring the constant offsets due to solvation, so the origin of the energy scale is arbitrary. In Figure 1, we ordered the sites according to their binding energies. For all of the nanocrystals examined, the energy of the nanocrystal−ligand bond increases by large jumps for certain classes of surface sites, with comparable plateaus having similar energies. We have plotted the spatial distribution of these surface sites in Figure 2. The distribution of these sites remains similar on the various facets as we increase the size of the nanocrystal. As the nanocrystal size increases, we note a reduction in the proportion of surface sites with the lowest energy, from 80%, 70%, 65%, to 64%. As shown in Figure 2, the distribution of the different energy surface sites appears to have a consistent pattern for all of the sizes of nanocrystals. Mind that only Cd atoms will be passivated by MPOH. We find that all of the Cd atoms with one dangling (i.e., nonsemiconductor attached) bond, regardless of the number of dangling bonds on the adjacent Se atoms, are all low binding energy sites. For Cd atoms with two dangling bonds, those whose both nearest-neighbor Se atoms have only one dangling bond each are low-energy sites. Approximately two-thirds of the higher energy sites occur on Cd atoms with two dangling bonds, in which none of the nearest-neighbor Se atoms have dangling bonds, and the remaining third occur on sites in which only one nearest-neighbor Se atom has one dangling bond, and the other Se has no dangling bonds. However, some of the low-energy binding sites occur on these two types of Cd atoms as well, so this type of nearest-neighbor environment classification does not completely characterize the different types of sites. The average ligand binding energy calculated for the lowest energy plateau increases in magnitude (i.e., becomes more negative) by 0.4 eV with the addition of each monolayer, which is opposite to the trend observed in experiment. Thus the change in the experimental binding energy does not come from the change of the plateau energy due to overall size effects. This suggests that the experimental difference between different nanocrystals may be a geometric (rather than electronic structure) effect, resulting from changes in the ratio of different surface facets (hence the ratio of different binding sites) when the size of the nanocrystal is changed.

Core/shell nanocrystals[23] may be used to test the relative importance of surface structure and band gap, since the band gap may be changed by modifying the core size, while leaving the surface structure intact. We performed ligand binding calculations on CdSe/CdS core/shell nanocrystals with a fixed total diameter of 4.1 nm, varying the CdSe core diameter to 0.9, 1.8, and 2.6 nm (corresponding to 4, 3, and 2 monolayer thick CdS shells, respectively), with calculated band gaps of 2.397, 2.285, and 2.211 eV, respectively. The results of our ligand binding calculations are shown in Figure 1b. We make several general observations. First, the fraction of low-energy sites is approximately the same for each of the three cases, with a slight shift to lower f_a for the smallest (0.9 nm diameter) core, which has the largest band gap. Second, as with the pure CdSe nanocrystals described above, the average of the first-plateau ligand binding energies becomes stronger as the core size is increased, which is contrary to the band gap−binding relation observed in experiment. The distribution of the site energies on the surface is shown in Figure 3; we have only depicted the 2.6 nm core diameter case, as the other two are quite similar. Here we distinguish only three different types of binding sites for the core/shell nanocrystals, as opposed to the four different types of sites distinguished in the solid CdSe nanocrystal. Compared to the similar plot for the 4.1 nm diameter CdSe nanocrystal, shown in Figure 2, the differences appear at the corners of the nanocrystal facets. The distribution of high- and low-energy surface sites, with respect to the local semiconductor environment, is qualitatively the same as described above for the pure CdSe nanocrystals.

As an alternative to the HSAB model, we propose another model to explain the results of Aldana et al. We assume that a certain fraction of the total number of cadmium surface, f_c, must be ligand passivated for the nanocrystal to remain in solution, independent of the nanocrystal diameter. The fraction of the surface that is passivated, f_p, depends on both the fraction of available surface Cd sites, f_a, which are in the low binding energy plateau (white spheres in Figure 2) (i.e., assuming the

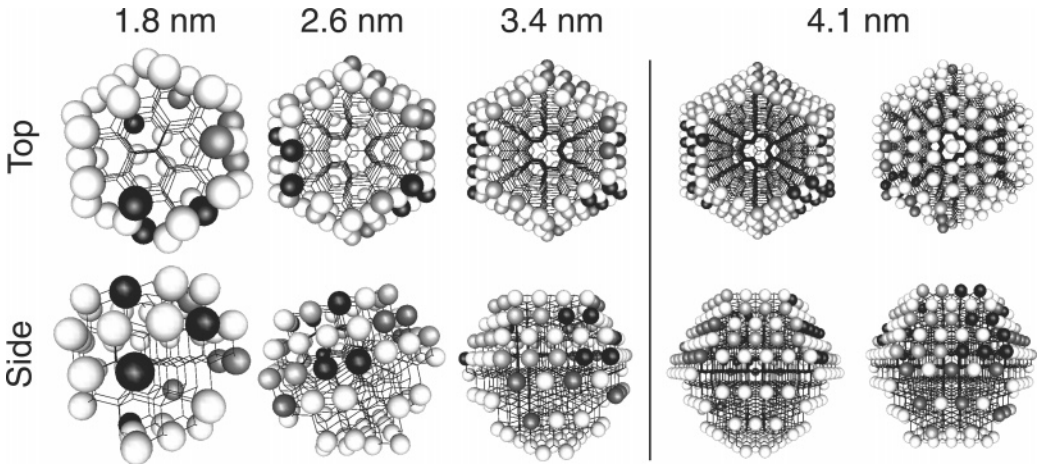

Figure 2. Illustration of the distribution of the types of binding sites on CdSe nanocrystals. Only the surface Cd atoms are passivated by MPOH and are shown here, with the color corresponding to the energy plateaus of Figure 1a. White corresponds to the low-energy plateau, and black to the highest energy plateau, with the dark and light gray indicating intermediate values. The top row shows a (Se-rich) top view of the nanocrystals; the bottom row shows a side view of each nanocrystal. For the 4.1 nm diameter nanocrystal, all sides are shown.

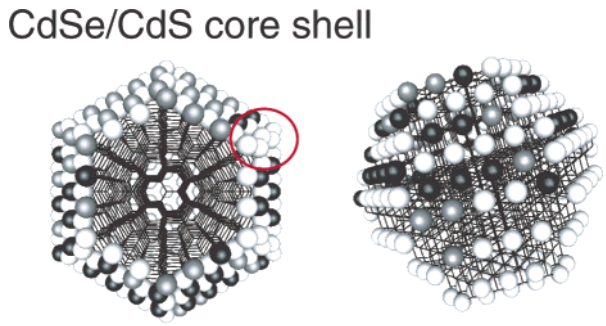

Figure 3. Distribution of MPOH binding energies on the surface sites on the 2.6 nm diameter CdSe/0.7 nm thick CdS core/shell nanocrystal; the 0.9 and 1.8 nm diameter CdSe core have essentially the same distribution. White spheres indicate the lowest energy plateau (in Figure 1b), gray the second plateau, and black the remaining highest energy sites. Compared to the pure CdSe nanocrystal in Figure 2, the corner attachment sites (one of which is circled in red) are changed in energy.

higher plateaus are too weakly bound to contribute), and the pH of the solution (which affects the number of ligands available for surface binding). When $f_p < f_c$, the nanocrystal precipitates out of solution; from the experimental observation, at least 80% of the surface ligands are removed when the nanocrystals are precipitated. Since the smaller nanocrystals have a larger fraction of the surface in this low binding energy plateau, this gives them an additional reservoir of sites to maintain their solubility, thus enabling them to remain in solution at lower pH than the larger nanocrystals. Comparing panels a and b in Figure 1, the overall shift in f_a observed for the CdSe/CdS core shell nanocrystals is comparable to that for the 2.6 nm diameter CdSe nanocrystals; by this model, both should have a similar precipitation pH. In the experimental results shown in Figure 5 of Aldana et al.,[11] the 3.8 nm diameter CdS nanocrystal was observed to have a precipitation pH similar to that of the 2.8 nm diameter CdSe nanocrystal.

More detailed theoretical and experimental investigations will be needed to confirm or disprove the above model. In particular, the above model may be inconsistent with one aspect of the experimental results. In the experiment, for a given sized quantum dot, none of the nanocrystals are precipitated until the pH value drops below a critical value, at which point all of the nanocrystals are precipitated out. If the pH value controls the percentage of the surface site passivation, the transition might be more gradual (due to the small number of sites on the surface of the nanocrystal). This might open up another explanation, that there is a size dependence of the binding energy due to other effects which were not included in our calculation, e.g., steric hindrance or local charging effects. Assuming spherical quantum dots, the surface curvature is inversely proportional to the nanocrystal radius. As a result, larger ligand side chains would be less crowded on the smaller nanocrystals, and thus steric effects would favor the formation of bonds to the smaller nanocrystals. This mechanism has been observed to result in the size-dependent reactivity of gold nanoparticles.[24,25] However, the experiments of Aldana et al.[11] using longer chain ligands seemingly found no evidence for steric effects on the ligand binding. Another possibility is the role of charge effects on the nanocrystal/ligand complex. For example, a negatively charged thiolate species could be compensated by an equal-magnitude positive charge on the nanocrystal surface, so as to achieve the overall charge neutrality of the nanocrystal−ligand complex observed experimentally. The electrostatic binding energy between the ligand and the nanocrystal might very well depend on the nanocrystal size. No matter what the final explanation for the experiment is, our calculations serve to rule out the binding energy−band gap dependence that was originally suspected.

IV. Conclusion

We have performed atomistic semiempirical quantum mechanical calculations on the interaction between CdSe and CdSe/CdS core/shell nanocrystals and MPOH. Our results suggest that the correlation between the binding energy and the nanocrystal band gap noted in the experiment is coincidental. From our results, we propose an alternative model for the size-dependent solubility experiments of Aldana et al., in which the solubility behavior is described by the fraction of low energy binding surface sites; we find that the ratio of the number of these sites to the total number of sites decreases as the nanocrystal becomes larger due to geometric effects. Experiments with core/shell nanocrystals would provide a clear test of this model, and distinguish the role of surface sites from band gap. Similarly, rod-shaped nanocrystals[26] will necessarily have a different distribution of low-energy ligand-binding sites on the surface. However, rods with different aspect ratios can have a similar band gap, but will have a very different fraction of low-energy sites, and thus, could also be used to test whether band gap or surface features dominate. Finally, further theoreti-

cal work including self-consistent charging in the EHT model or using higher level semiempirical and ab initio Hamiltonians would help clarify the role of surface charging effects.

Acknowledgment. This work was supported by the U.S. Department of Energy under Contract No. DE-AC02-05OH11231 and by the DOE-SC-BES Materials Sciences and Engineering Division. The calculations were performed with use of the resources of the National Energy Research Scientific Computing Center. We thank a referee for clarifying the steric and counterion experiments performed in the steady-state titration study.

References and Notes

(1) Alivisatos, A. *J. Phys. Chem.* **1996**, *100*, 13226.
(2) Jeong, S.; Achermann, M.; Nanda, J.; Ivanov, S.; Klimov, V. I.; Hollingsworth, J. A. *J. Am. Chem. Soc.* **2005**, *127*, 10126.
(3) Derfus, A. M.; Chan, W. C. W.; Bhatia, S. N. *Nano Lett.* **2004**, *4*, 11.
(4) Rabani, E. *J. Chem. Phys.* **2001**, *115*, 1493.
(5) Gurin, V. S. *J. Phys.*: *Condens. Mater.* **1994**, *6*, 8691.
(6) Gurin, V. S. *J. Phys. Chem.* **1996**, *100*, 869.
(7) Nosaka, Y.; Tanaka, H. *J. Phys. Chem. B* **2002**, *106*, 3389.
(8) Eichkorn, K.; Ahlrichs, R. *Chem. Phys. Lett.* **1998**, *288*, 235.
(9) Puzder, A.; Williamson, A. J.; Zaitseva, N.; Galli, G.; Manna, L.; Alivisatos, A. P. *Nano Lett.* **2004**, *4*, 2361.
(10) Manna, L.; Wang, L.-W.; Cingolani, R.; Alivisatos, A. P. *J. Phys. Chem. B* **2005**, *109*, 6183.
(11) Aldana, J.; Lavelle, N.; Wang, Y.; Peng, X. *J. Am. Chem. Soc.* **2005**, *127*, 2496.
(12) Parr, R. G.; Yang, W. *Density-Functional Theory of Atoms and Molecules*; Oxford Science: Oxford, UK, 1994.
(13) Wang, L.-W.; Li, J. *Phys. Rev. B* **2004**, *69*, 153302.
(14) Li, J.; Wang, L.-W. *Appl. Phys. Lett.* **2004**, *84*, 3648.
(15) Huang, X.; Lindgren, E.; Chelikowsky, J. R. *Phys. Rev. B* **2005**, *71*, 165328.
(16) Martins, J. L.; Zunger, A. *Phys. Rev. B* **1984**, *30*, 6217.
(17) Pryor, C.; Kim, J.; Wang, L. W.; Williamson, A. J.; Zunger, A. *J. Appl. Phys.* **1998**, *83*, 2548.
(18) Hoffmann, R. *J. Chem. Phys.* **1963**, *39*, 1397.
(19) Whangbo, M.-H. *Theor. Chem. Acc.* **2000**, *103*, 252.
(20) Landrum, G. A. *Yet another extended Hückel molecular orbital package* (*YAeHMOP*); Cornell University: Ithaca, NY, 1997.
(21) Clementi, E.; Roetti, C. *At. Data Nucl. Data Tables* **1974**, *14*, 177.
(22) Cerdá, J.; Soria, F. *Phys. Rev. B* **2000**, *61*, 7965.
(23) Peng, X.; Schlamp, M. C.; Kadavanich, A. V.; Alivisatos, A. P. *J. Am. Chem. Soc.* **1997**, *119*, 7019.
(24) Templeton, A. C.; Hostetler, M. J.; Kraft, C. T.; Murray, R. W. *J. Am. Chem. Soc.* **1998**, *127*, 1906.
(25) Lucarini, M.; Franchi, P.; Pedulli, G. F.; Gentilini, C.; Polizzi, S.; Pengo, P.; Scrimin, P.; Pasquato, L. *J. Am. Chem. Soc.* **2005**, *127*, 16384.
(26) Peng, X.; Manna, L.; Yang, W.; Wickham, J.; Scher, E.; Kadavanich, A.; Alivisatos, A. P. *Nature* **2000**, *404*, 59.